UNIVERSITÀ DEGLI STUDI DI BRESCIA

DIPARTIMENTO DI INGEGNERIA CIVILE ARCHITETTURA TERRITORIO AMBIENTE E DI MATEMATICA - D I C A T A M

TECHNICAL REPORT N. 1

ANNO 2018

Design and assessment of adjustable telescopic props with innovative shape

G. Fantoni[2], A. Salvadori[1], E. Marchina [1]

[1]*Dipartimento di Ingegneria Civile, Architettura, Territorio, Ambiente e di Matematica - Università degli Studi di Brescia*
[2]*Collaboratrice*

TECHNICAL REPORT

DEPARTMENT OF CIVIL ENGINEERING,

ARCHITECTURE, LAND, ENVIRONMENT AND MATHEMATICS

I Rapporti Tecnici del Dipartimento di Ingegneria Civile, Architettura, Territorio, Ambiente e di Matematica dell'Università degli Studi di Brescia raccolgono i risultati inerenti le ricerche svolte presso il Dipartimento stesso.

I Rapporti Tecnici sono pubblicati esclusivamente per una prima divulgazione del loro contenuto in attesa di pubblicazione su riviste nazionali ed internazionali

The Technical Reports of the Civil Engineering, Architecture, Land, Environment and Mathematics Department of the University of Brescia are intended to record research carried out by the same Department.

The Technical Reports are issued only for dissemination of their content, before publication on national or international journal.

Direttore responsabile prof. Giovanni PLIZZARI
Autorizzazione del Tribunale di Brescia 21.3.1991 n. 13
Comitato di Redazione: Baldassare BACCHI, Giorgio BERTANZA, Angelo CARINI, Angelo CIRIBINI, Lucia GASTALDI, Roberto RANZI, Paolo SECCHI, Maurizio TIRA

La presente pubblicazione di N. 2+12 pagine costituisce articolo, in attesa di pubblicazione, stampato in proprio, a fine concorsuale ai sensi delle "informazioni e chiarimenti" per l'applicazione dell'art. 8 del D.P.R. 252/2006.

Design and assessment of adjustable telescopic props with innovative shape.

G. Fantoni, A. Salvadori, E. Marchina

DICATAM - Dipartimento di Ingegneria Civile, Architettura, Territorio, Ambiente e di Matematica

Università di Brescia, via Branze 43, 25123 Brescia, Italy

Tel: +39-030-3711239; Fax: +39-030-3711312; alberto.salvadori@unibs.it

Abstract

As shown in [1], the design of optimal props (in terms of weight) that conform to the European standard EN 1065 is not a straightforward task. For some classes of props, when the collapse mechanism is the failure of the prop base, large tubes thicknesses or large tubes diameters are required to keep the failure mechanism under control, although the substantial strength of the tubes remains unexploited. This observation motivates the seek for innovative shapes. The present work aims at showing a new proposal of efficient design of props in agreement with the standard EN 1065. Theoretical and numerical analysis are carried out in order to identify the effective gain of weight of this new design configuration.

1 Introduction

An adjustable telescopic prop is a structural member normally used as provisional vertical support in construction works. It consists in two tubes which are telescopically displaceable within each other. Currently the European props production is ruled by the standard EN 1065 for steel props, and by EN 16031 for aluminum props.

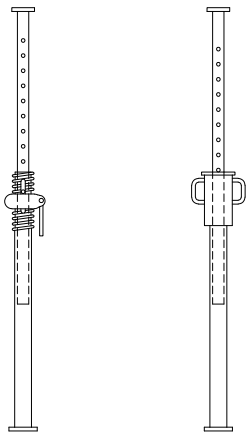

Figure 1: The usual design for steel props.

In a recent publication [1] the prop design and failure mechanisms were investigated. A computer code, named PrOptmizer, descended from [1] and was capable to optimize the design of props in the usual configuration, i.e. built with two singles tubes as in figure 1, in terms of weight accordingly to the European standard EN 1065. The optimal prop that results from design is the lightest among a large customized data set of props that are safe with respect to all the collapse mechanisms defined in EN 1065.

An accurate analysis of the outcomes of optimized props revealed that there is no poor performance when the most dangerous failure mechanism is the flexural collapse, since the base of a prop contributes

secondarily to the prop poundage. On the contrary, when the most dangerous mechanism is the collapse of the bases, either the diameter or the thickness of the tubes must be severely increased to provide the base with sufficient strength, in detriment of weight and material performances. This event occurs regularly in long props.

For the sake of confidentiality, a design of a product of interest for real industry cannot be reported here. Nevertheless, the statement above (and with it also the purpose of the paper) can be illustrated by the following benchmark. Consider a prop of class D55, assuming the inner tube upwards. Materials for the tubes are $S235$ (Young modulus $E = 210\,\text{GPa}$, yield strength $f_y = 235\,\text{MPa}$) for the outer tube and $S355$ for the inner one (yield strength $f_y = 395\,\text{MPa}$ after cold forming). Geometry parameters read: $l_{max} = 5500\,\text{mm}$; holes diameter $d_h = 15.5\,\text{mm}$; distance between holes $a_h = 100\,\text{mm}$; base thickness $t = 8\,\text{mm}$.

Select furthermore the following parameters for the tubes. *Outer tube*: outer diameter $D_o = 76\,\text{mm}$; thickness $t_o = 3.1\,\text{mm}$; length $l_o = 3100\,\text{mm}$. *Inner tube* : outer diameter $D_i = 62\,\text{mm}$; thickness $t_i = 7\,\text{mm}$; length $l_i = 3200\,\text{mm}$.

The *weight* of this prop is 49.47 kg. Although far from being optimal in weight, the prop is well designed; figure 2 shows that the safety factor amounts to 1.01. Nevertheless, a more careful investigation of the

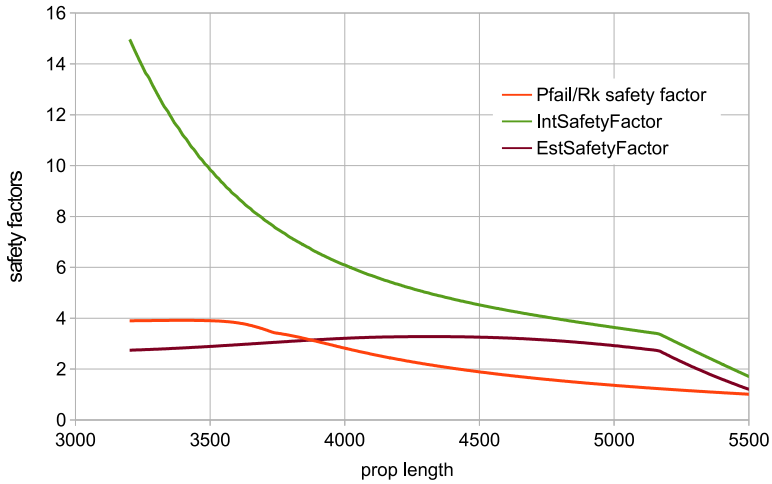

Figure 2: Safety factors plot for the benchmark prop.

bending moment - see also figure 3 - shows that material in the inner tube is not adequately utilized, since the flexural strength remains much higher than the bending moment. The collapse mechanism is in fact the failure of the prop base and tube thicknesses are very high, in spite the large flexural strength of the tubes remains unexploited.

When the collapse mechanism is the failure of the prop base, therefore, the classical shape may not allow an optimal design in terms of weight. Tubes thicknesses or diameters must be significantly increased to comply with the design requirements of the standard, but design does not take advantage of their strength. Innovative shapes, for instance by welding at the end of the two tubes an enlarged part - see figure 4, are called to alleviate the waste of materials and performances.

This note is organized as follows. In Section 2, the requirements and guidelines for the design of prop tubes are summarized: the criteria for the evaluation of the ultimate bearing capacity, the structural models and the collapse mechanisms are elucidated. An algorithm for the evaluation of innovative props carrying capacity is detailed in Section 3. Following the standard EN1065, the algorithm distinguishes "three phases" of the structural evolution and allows the evaluation of the Eulerian critical loads and of the transition loads between the three static schemes. The algorithm is applied to the design of a D55 prop with enlarged bases in section 4, and the paper winds up comparing the performances between the already depicted usual design and the innovative shape.

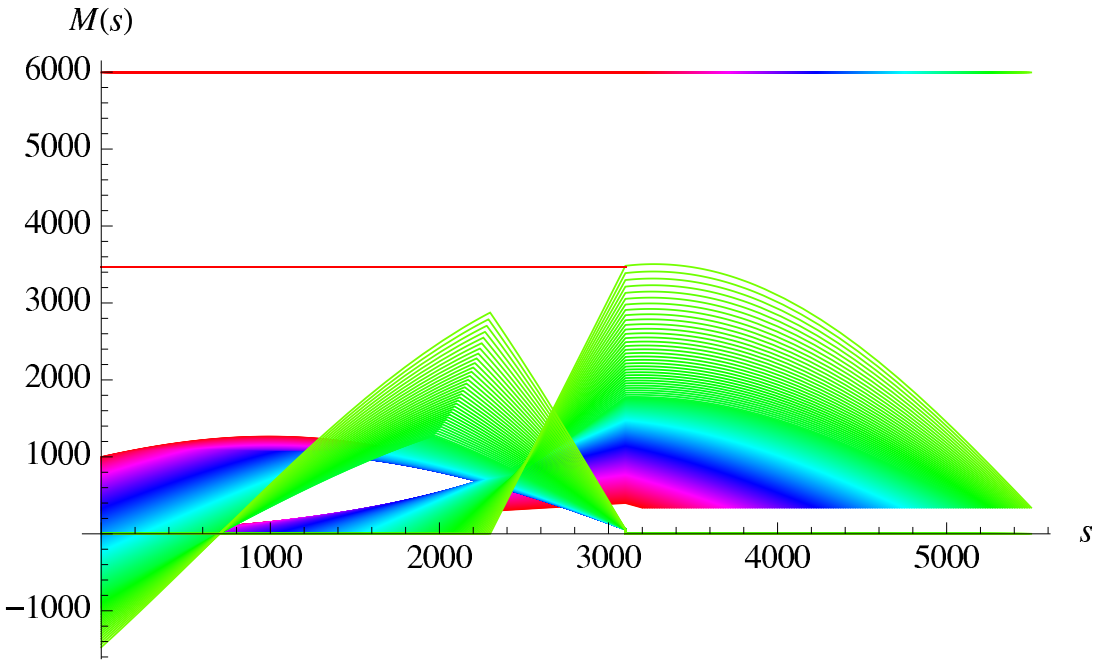

Figure 3: Envelope of bending moment and flexural strength of the tubes at different extension lengths. Straight lines above depict the flexural strength of tubes, the highest corresponds to the inner tube.

Figure 4: A 3D rendering of AB part, welded to the endplate and to the outer tube.

2 Essentials of the standard EN 1065

2.1 Classification

Five classes of props (A-E) are defined. For each class y the standard establishes the loading capacity $R_{y,k}$ at the current extension l:

$$R_{A,k} = 51,0\frac{l_{\max}}{l^2} \leq 44,0\,kN\,; \qquad R_{B,k} = 68,0\frac{l_{\max}}{l^2} \leq 51,0\,kN \tag{1}$$

$$R_{\mathsf{C},k} \quad = \quad 102,0\frac{l_{\max}}{l^2} \leq 59,5\,kN\,; \qquad R_{\mathsf{D},k} = 34,0\,kN\,; \qquad R_{\mathsf{E},k} = 51,0\,kN \tag{2}$$

The ultimate strength $R_{\mathsf{y},act}$ of a prop must exceed the loading capacity $R_{\mathsf{y},k}$ at any extension l.

2.2 Materials and components

Mechanical properties of the material must be in agreement with the existing European Standards and all materials must be protected against corrosion. The tubes cross section must be selected according to the international reference standards. The nominal thickness must not be smaller than 2.6 mm for props in classes B, C, D, E, while for A class props nominal thickness is required to be grater or equal to 2.3 mm, tolerances included. The overlap between the inner and the outer tube has to be at least equal to 300 mm. A distance between the end of the outer tube and the internal part of the prop plate at least equal to 100 mm is mandatory to protect against hand crushing. No-slipping devices are compulsory to avoid the inner and the outer tubes to separate one another.

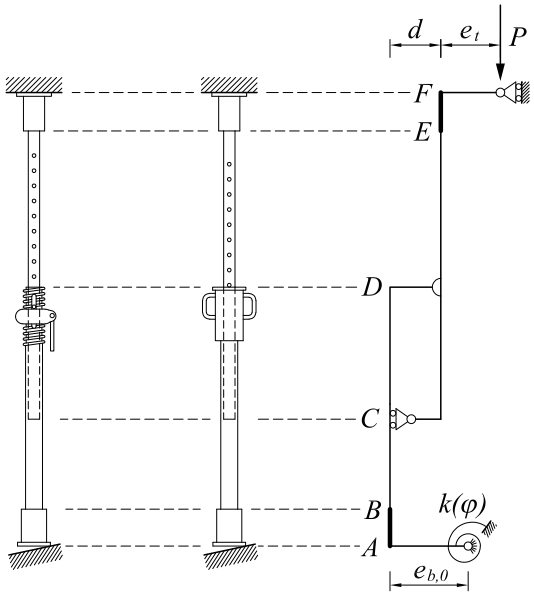

Figure 5: Structural model for prop design. Distance d is actually vanishing: it must be conceived as a graphical artefact. Constitutive law $k(\varphi)$ is described in figure 6.

2.3 Design requirements

2.3.1 Structural model

The structural model of a prop with an enlarged base is not included in the standard EN 1065. A proposal of structural model that emanates from EN 1065 is shown in figure 5. The tubes overlapping zone is modeled by the contemporary presence of the inner and outer tubes, relatively joined by a frictional constraint (located at point C at the end of the inner tube) and a hinge (at point D, at the end of the outer tube). As done in [1], a perfect constraint has been taken into account, as shown in figure 5. At the bases, two tubes with a larger diameter are welded: they correspond to parts AB and EF. The configuration of inner tube downward has been verified as well.

2.3.2 Defects

Imperfections must be considered. They are taken into account in the structural model by means of: i) a load eccentricity $e_t = 10\,\text{mm}$ - chosen independently on the geometry of the prop and of its base; ii) an

inclination angle $\Delta\varphi_0$ due to the tubes spacing and to the length of the actual overlapping zone[1]; iii) an initial sinusoidal deformation with a maximal inflection of $\frac{l}{500}$, being l the actual prop length.

2.3.3 Collapse mechanisms

The standard EN 1065 considers three failure mechanisms: *buckling of the tubes*, *flexural collapse*, and *failure of the prop base*.

Props must be designed preventing the *buckling of the tubes*, by evaluating the influence of the configuration on the internal actions predicted by the second order elastic beam theory, assuming the material to be linear without limitation of stresses and strains in magnitude.

Flexural collapse takes place when the bending moment overcomes the plastic flexural strength $M_{pl,N}$. According to the standard EN1065 the plastic flexural strength is estimated as:

$$M_{pl,N} = M_{pl} \cos\left(\frac{\pi}{2}\frac{N}{N_{pl}}\right) \tag{3}$$

thus accounting for axial load (N) effects. In the previous equation, M_{pl} represents the plastic flexural strength of the tube, while N_{pl} is the axial compressive strength of the tube.

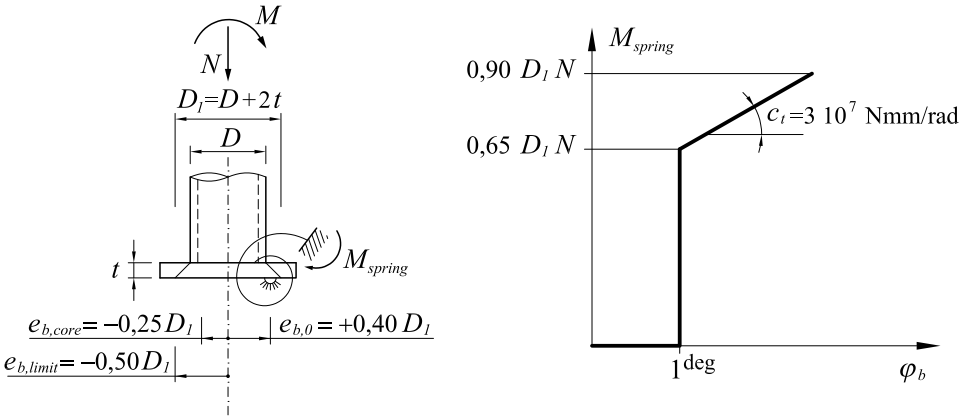

Figure 6: Prop base modeling by means of torsional constraint M_{spring} versus φ_b.

The standard EN 1065 describes the progressive *failure of a real support at the base of a prop* moving from an initial, horizontal position to a final, slanted configuration. The state of the prop base shepherds the sequence of three structural schemes in figure 5.

In the first scheme the prop base is free to rotate. The prop torsional constraint corresponds to a standard hinge: an eccentricity $e_{b,0} = 0,40\, D_1$ is devised[2] . When rotation φ_b reaches 1^{deg}, the standard conventionally switches to the second static scheme. The constraint at the base of the prop behaves like a rigid joint and any further rotation is prevented until the ratio $\frac{M_{spring}}{N}$ reaches the core eccentricity $e_{b,0} + e_{b,core}$ (where $e_{b,core} = -0,25\, D_1$).

The third static system is reached when external actions induce a ratio $\frac{M_{spring}}{N} \geq (e_{b,0} + e_{b,core})$. The constraint at the base of the prop is modeled like a spring, whose moment M_{spring} increases linearly with the base rotation increment with stiffness $c_t = 3 \times 10^7 \text{Nmm}\,\text{rad}^{-1}$ up to a failure value which corresponds to an eccentricity $e_{b,limit} = -0,50\, D_1$.

In the presence of innovative, tailored shapes of the ends of the tubes and of their connections with the bases, the standard should consider the eventuality of increasing the base stiffness c_t.

[1] $\Delta\varphi_0$ must be evaluated from the nominal device sizes; an example is shown in the following section.

[2] For planar bases, the plate thickness t can be considered as a part of the effective diameter $D_1 = D + 2t$ having denoted with D the outer diameter of the downward tube

3 An algorithm for ultimate strength assessment.

A "three steps" algorithm - one for each static scheme of figure 5 - appears to be efficient for props design. At any given prop geometry, three transition loads are defined, one for each step of the algorithm; $P_{1^{\deg}}$ enshrines the passage between the first and the second static scheme; incrementing the external load the amount P_{lim} is reached, which is defined as the transition load between the second and the third static scheme. At last, when P is equal to P_{fail}, the load carrying capacity of the prop is assumed to be exhausted. Figure 7 summarizes this path of reasoning.

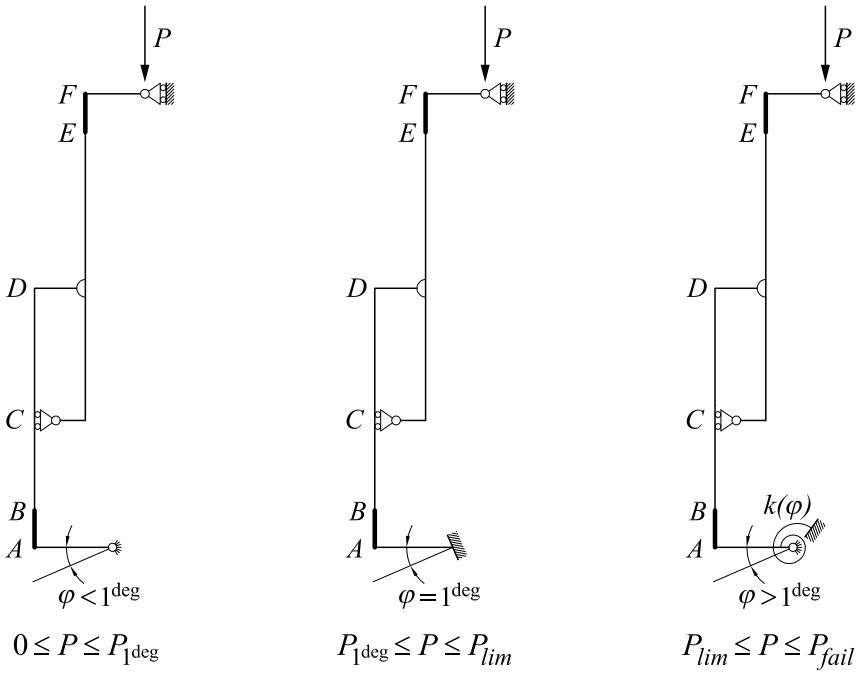

Figure 7: External load intervals for the proposed algorithm. $P_{1^{\deg}}$, P_{lim} and P_{fail} depend on geometry and on the material properties.

All calculations to evaluate $P_{1^{\deg}}$, P_{lim} and P_{fail} have been performed according to figure 7. The structural scheme separates the outer from the inner tube and subdivides them both in parts. The AC interval is the non-overlapping part of the downward tube, whereas CD is its overlapping counterpart. Similarly, DF is the non-overlapping part of the upward tube, whereas DC is its overlapping part. Portions AB and EF represent the enlarged tubes welded to the endplate - see figure 4.

Functions $v_n(s)$ with $n = AB, BC, CD, DC, ED, EF$ describe the prop axis (small) deflection in each part. EN 1065 standard defines the total deflection $v_n(s)$ as the sum of the elastic contribution $v_n^{el}(s)$, of the initial sinusoidal deflection $v_n^{sin}(s)$ and of the deflection $v_n^{inc}(s)$ due to the inclination angle $\Delta\varphi_0$. The elastic contribution $v_n^{el}(s)$ can be evaluated from Bernoulli-Navier equations, that read:

$$\frac{d^2\, v_n^{el}}{d\, s^2} = -\frac{M(s,P)}{E\, I_n} \quad , \qquad n = AB, BC, CD, DC, ED, EF \tag{4}$$

Continuity at each intersection of the six parts together with the constraints provide the required 12 boundary conditions in the first static system and the mandatory 13 in the second and third ones. A linear system of equations can be thus be written, which is uniquely solvable when loads P are below the Eulerian bifurcation amount.

After solving the linear system of equations the elastic displacement $v_n^{el}(s)$ can be recovered as a function of the external load P. If the nominal strength $R_{y,k}$ - evaluated from equations (1-2) - is lower then $P_{1^{\deg}}$,

the bending moment must be deduced from the first static system; if $P_{1^{\deg}} \leq R_{y,k} \leq P_{lim}$ it turns out from the second static scheme and if $P_{lim} \leq R_{y,k} \leq P_{fail}$ from the third one.

Once the bending moment $M(s, P)$ has been deduced from the proper structural scheme, safety against flexural collapse requires that $M(s, P) \leq M_{pl,N}$ for any $0 \leq s \leq l$, with $M_{pl,N}$ evaluated by (3). Moreover, structural stability requires that $R_{y,k} < P_E$ where P_E denotes the Eulerian load of the scheme pertaining to $R_{y,k}$ - see figure 7.

If $P_{fail} \leq R_{y,k}$ then the prop cannot prevent to fail due to the exhausted support strength. It is exactly under this condition that the strength of the tubes may not be fully exploited and the design not be optimal in terms of props weight.

4 An example

The ultimate strength of an enlarged steel prop of class D55 is evaluated according to the procedure described in section 3, assuming $l = l_{max} = 5500$mm and the inner tube upwards. Materials for the tubes are $S235$ (Young modulus $E = 210\,\text{GPa}$, yield strength $f_y = 235\,\text{MPa}$) for AD part and $S355$ for the CF part (yield strength $f_y = 395\,\text{MPa}$ after cold forming). Geometry parameters read - see also figure 9: maximal extension $l_{max} = l_o + l_m + l_i = 5500\,\text{mm}$; overlapping length $l_m = 800\,\text{mm}$; holes diameter $d_h = 15.5\,\text{mm}$; distance between holes $a_h = 100\,\text{mm}$; base thickness $t = 8\,\text{mm}$. *Outer tube BD* parameters: outer diameter $D_o = 76\,\text{mm}$; thickness $t_o = 2.9\,\text{mm}$; length $l_o + l_m - l_{AB} = 2800\,\text{mm}$. *Inner tube CE* parameters: outer diameter $D_i = 62\,\text{mm}$; thickness $t_i = 6.6\,\text{mm}$; length $l_i + l_m - l_{EF} = 2900\,\text{mm}$. *Enlarged tube AB* parameters: outer diameter $D_o = 91\,\text{mm}$; effective diameter at the base $D_{o1} = D_o + 2t = 107\,\text{mm}$; thickness $t_o = 2.6\,\text{mm}$; length $l_{AB} = 300\,\text{mm}$. *Enlarged tube EF* parameters: outer diameter $D_i = 77\,\text{mm}$; effective diameter at the base $D_{i1} = D_i + 2t = 93\,\text{mm}$; thickness $t_i = 2.6\,\text{mm}$; length $l_{EF} = 300\,\text{mm}$. It is interesting to check the influence of the length of EF part in the weight of the prop: indeed, the small thickness of this enlarged part allows to design a lighter prop.

l_{EF}[mm]	Weight of the prop [kg]
300	45.73
500	44.88
750	43.82
1000	42.76
1100	42.33
1200	41.91

Table 1: Influence of EF part on the weight of the prop

Parameters $d_p = 66.6$mm e $d_s = 65.6$mm (see figure 9) play a basic role in the evaluation of angle $\Delta\varphi_0$ between the tubes; making reference to figure 8, *the deflection due to the inclination angle* $\Delta\varphi_0$ - denoted with $v_n^{inc}(s)$ - reads:

$$\begin{aligned} v_{AB}^{inc}(s) &= m_e \cdot s \\ v_{BC}^{inc}(s) &= m_e \cdot s \\ v_{CD}^{inc}(s) &= m_e \cdot s \\ v_{DC}^{inc}(s) &= m_i \cdot (l_{max} - s) \\ v_{ED}^{inc}(s) &= m_i \cdot (l_{max} - s) \\ v_{EF}^{inc}(s) &= m_i \cdot (l_{max} - s) \end{aligned}$$

where $m_e = \tan\varphi_A \cong \varphi_A = 0.00229091 rad$ and $m_i = \tan\varphi_F \cong \varphi_F = 0.00220909 rad$ (see figure 9). As the standard does not provide instructions to evaluate $\Delta\varphi_0$, the approach followed in [1] is taken. It is summarized in appendix A.

The initial sinusoidal deflection $v_n^{sin}(s)$, with notation of figure 5, reads:

$$v^{sin} = \frac{l_{max}}{500} \sin \frac{\pi}{l_{max}} s \tag{5}$$

The tubes geometry has an impact on the inertia moments of the tubes section. For the outer tube, the section is a ring with inertia $I_{out} = I_{BC} = 445546\,\text{mm}^4$. For the inner one, the standard EN 1065 provides

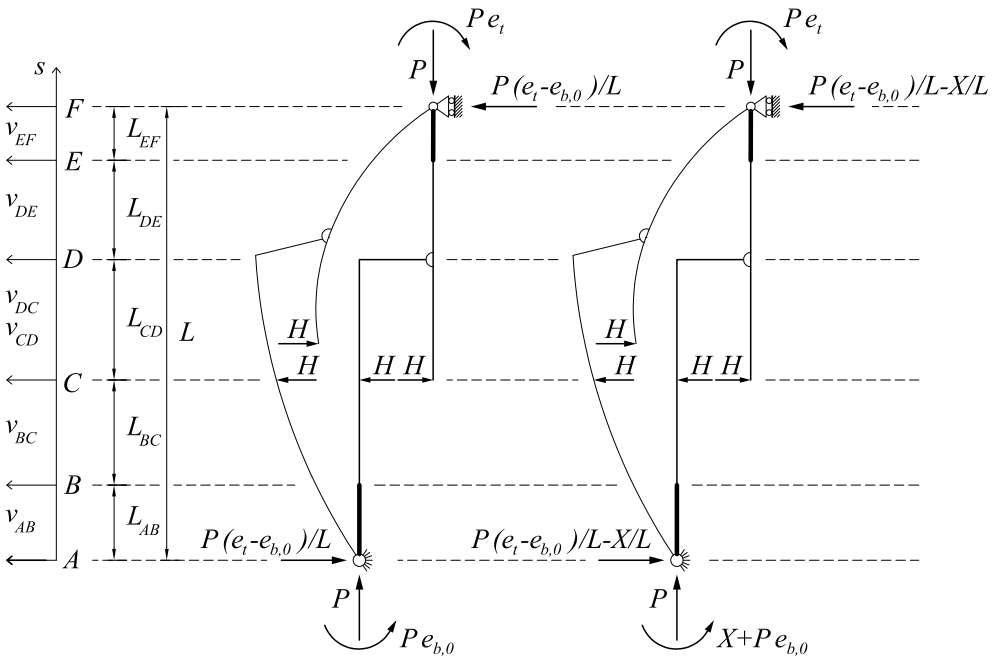

Figure 8: Notation and elastica configurations.

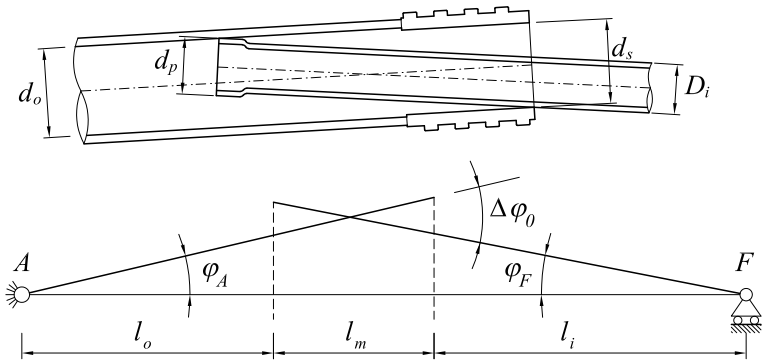

Figure 9: Modeling of the two tubes overlapping. Here: $\Delta\varphi_0$ is the angle between the tubes; l_m the overlapping length; d_s inner diameter at the end of the outer tube; d_p outer diameter at the end of the inner tube

a special procedure for inertia evaluation, summarized in the Appendix in [1]. $I_{in} = I_{ED} = 383427\,\mathrm{mm}^4$ comes out. The inertia for the enlarged part AB amounts at $I_{AB} = 705936\,\mathrm{mm}^4$, while for EF part $I_{EF} = 421000\,\mathrm{mm}^4$.

In the second and third static schemes, X stands for the over-constraint moment at the prop base. The reaction force H has to be evaluated in the deformed configuration as a function of the external load P, of deflection $v_{ED}(L_{AD})$ at point D and eventually of X.

In the first static scheme - $0 \le P \le P_{1^{\deg}}$ - the Bernoulli-Navier equations (4) read:

$$v''_{AB}(s) + \alpha^2_{AB} v_{AB}(s) \quad = \quad -\alpha^2_{AB}\left(m_e\, s + (e_t - e_{b,0})\frac{s}{l_{max}} + e_{b,0}\right) - \frac{\alpha^2_{AB}\, l_{max}}{500}\sin\pi\,\frac{s}{l_{max}} \tag{6a}$$

$$
\begin{aligned}
v''_{BC}(s) + \alpha^2_{BC} v_{BC}(s) &= -\alpha^2_{BC}\left(m_e\, s + (e_t - e_{b,0})\frac{s}{l_{max}} + e_{b,0}\right) - \frac{\alpha^2_{BC}\, l_{max}}{500}\sin\pi\,\frac{s}{l_{max}} && \text{(6b)}\\
v''_{EF}(s) + \alpha^2_{EF} v_{EF}(s) &= -\alpha^2_{EF}\left(m_i\,(l_{max} - s) - (e_t - e_{b,0})\frac{l_{max} - s}{l_{max}} + e_t\right) - && \text{(6c)}\\
&\quad -\frac{\alpha^2_{EF}\, l_{max}}{500}\sin\pi\,\frac{s}{l_{max}} &&\\
v''_{ED}(s) + \alpha^2_{ED} v_{ED}(s) &= -\alpha^2_{ED}\left(m_i\,(l_{max} - s) - (e_t - e_{b,0})\frac{l_{max} - s}{l_{max}} + e_t\right) - && \text{(6d)}\\
&\quad -\frac{\alpha^2_{ED}\, l_{max}}{500}\sin\pi\,\frac{s}{l_{max}} &&\\
v''_{CD}(s) + \alpha^2_{BC} v_{CD}(s) &= -\alpha^2_{BC}\frac{l_{max}}{500}\sin\frac{s}{l_{max}}\pi - \alpha^2_{BC}\left(m_e\, s + (e_t - e_{b,0})\frac{s}{l_{max}} + e_{b,0}\right) && \text{(6e)}\\
&\quad +\alpha^2_{BC}\frac{s - L_{AC}}{L_{CD}}\left[\frac{l_{max}}{500}\sin\frac{L_{AD}}{l_{max}}\pi + m_i\, L_{DF} + e_t - \frac{L_{DF}}{l_{max}}(e_t - e_{b,0})\right. &&\\
&\quad \left.+v_{ED}(L_{AD})\right] &&\\
v''_{DC}(s) &= \frac{\alpha^2_{ED}}{L_{CD}}(L_{AC} - s)\left[\frac{l_{max}}{500}\sin\frac{L_{AD}}{l_{max}}\pi + m_i\, L_{DF} + e_t - \right. && \text{(6f)}\\
&\quad \left. -\frac{L_{DF}}{l_{max}}(e_t - e_{b,0}) + v_{ED}(L_{AD})\right] &&
\end{aligned}
$$

with $\alpha^2_{AB} = \frac{P}{EI_{AB}}$, $\alpha^2_{BC} = \frac{P}{EI_{BC}}$, $\alpha^2_{EF} = \frac{P}{EI_{EF}}$ e $\alpha^2_{ED} = \frac{P}{EI_{ED}}$. Twelve boundary conditions are required to solve problem (6):

$$
\begin{aligned}
&v_{AB}(0) = 0 && \text{(7a)}\\
&v_{AB}(L_{AB}) = v_{BC}(L_{AB}) && \text{(7b)}\\
&v_{BC}(L_{AB} + L_{BC}) = v_{CD}(L_{AB} + L_{BC}) && \text{(7c)}\\
&v_{CD}(L_{AB} + L_{BC}) = v_{DC}(L_{AB} + L_{BC}) && \text{(7d)}\\
&v_{CD}(L_{AB} + L_{BC} + L_{CD}) = v_{DC}(L_{AB} + L_{BC} + L_{CD}) && \text{(7e)}\\
&v_{DC}(L_{AB} + L_{BC} + L_{CD}) = v_{ED}(L_{AB} + L_{BC} + L_{CD}) && \text{(7f)}\\
&v_{ED}(L_{AB} + L_{BC} + L_{CD} + L_{ED}) = v_{EF}(L_{AB} + L_{BC} + L_{CD} + L_{ED}) && \text{(7g)}\\
&v_{EF}(0) = 0 && \text{(7h)}\\
&v'_{AB}(L_{AB}) = v'_{BC}(L_{AB}) && \text{(7i)}\\
&v'_{BC}(L_{AB} + L_{BC}) = v'_{CD}(L_{AB} + L_{BC}) && \text{(7j)}\\
&v'_{DC}(L_{AB} + L_{BC} + L_{CD}) = v'_{ED}(L_{AB} + L_{BC} + L_{CD}) && \text{(7k)}\\
&v'_{ED}(L_{AB} + L_{BC} + L_{CD} + L_{ED}) = v'_{EF}(L_{AB} + L_{BC} + L_{CD} + L_{ED}) && \text{(7l)}
\end{aligned}
$$

The limit load $P_{1^{\text{deg}}}$ for the first static scheme comes out after imposing the condition $v'_{AB}(0) = \frac{\pi}{180}$: it amounts to $P_{1^{\text{deg}}} = 10.68\,\text{kN}$. By imposing a null matrix determinant in the system of twelve equations (7a-7l) the critical load for analysis #1 turns out to be $P_{cr,1} = 31.06\,\text{kN} > P_{1^{\text{deg}}}$.

Using a similar path of reasoning, the second and the third static schemes have been solved: they require a further boundary condition because of the over-constraint. In the second scheme the rotation at the base must be one degree. In the third scheme, the moment at the base is related to the rotation in the spring by means of elasticity constant c_t - see figure 6:

$$
v'_{AB}(0) = \frac{\pi}{180}\,; \qquad v'_{AB}(0) = -\frac{X}{c_t} - \frac{(e_{b,0} + e_{b,core})\; P}{c_t} + \frac{\pi}{180} \qquad \text{(7m)}
$$

The transition between the second and the third scheme is stated by the condition

$$
v'_{AB}(0) = \frac{\pi}{180} \qquad \rightarrow \qquad X = -P\,(e_{b,0} + e_{b,core})
$$

that generates a $P_{lim} = 27.24\,\text{kN}$. The support strength of the prop is exhausted when $X = -P\,(e_{b,\text{lim}} + e_{b,0})$, that leads to $P_{fail} = 34.10\,\text{kN}$. By imposing a null matrix determinant in the system of thirteen boundary conditions (7), the critical loads for analyses #2 and #3 come out. They amount to $P_{cr,2} = 61.10\,\text{kN} > P_{lim}$ and $P_{cr,3} = 39.15\,\text{kN} > P_{fail}$. Since the transition loads are lower than the corresponding Eulerian load in every static scheme, the prop is adequately designed against the failure due to structural instability. Moreover, the value of P_{fail} is slightly higher than $R_{\text{D},k} = 34\,\text{kN}$:

$$R_{\text{D},k} = 34\,\text{kN} < 34.10\,\text{kN} = P_{fail} \tag{8}$$

That means that the prop is well designed, since it would be impossible to decrease any parameter of the prop without exhausting the support strength (which is the most common collapse mechanism for this class of props).

Finally, because $P_{lim} < R_{\text{D},k} < P_{fail}$, it is necessary to check that the bending moment due to $P = R_{\text{D},k}$ in analysis #3 is lower than $M_{pl,N}$ at all points of the prop. The plastic flexural strength, according to equation (3), amounts to $M_{pl,N,AB} = 4333\text{kNmm}$ for the enlarged tube AB, amounts to $M_{pl,N,EF} = 5266\text{kNmm}$ for the enlarged tube EF, amounts to $M_{pl,N,BD} = 3245\text{kNmm}$ for the outer tube and to $M_{pl,EC} = 5740\text{kNmm}$ for the inner one.

A plot of bending moment versus the plastic flexural strength is represented in figure 10: the curve lines represent the bending moment of the whole prop, while the straight lines represent the plastic flexural strength. It allows to conclude that, at the maximum extension, the analyzed prop is designed in agreement with standard EN 1065. The carrying capacity according to EN 1065 has to be tested at the minimum length and at the most unfavorable intermediate configuration as well. The same analyses have been repeated positioning the prop with the internal tube downward, and the transition loads measure: $P_{1^{\text{deg}}} = 10.46\,\text{kN}$; $P_{lim} = 27.11\,\text{kN}$; $P_{fail} = 34.63\,\text{kN} > R_{\text{D},k}$.

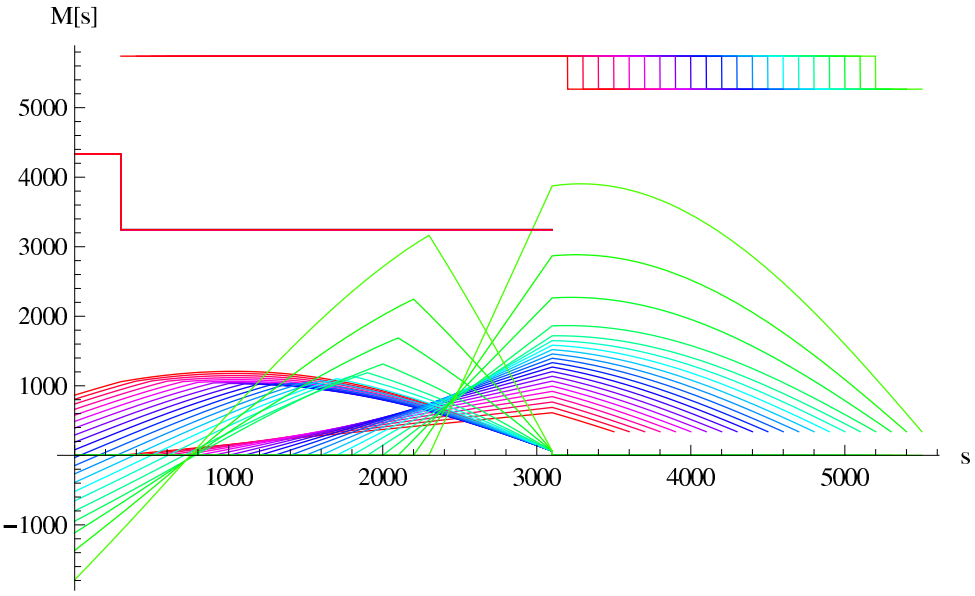

Figure 10: Comparison between the plastic flexural strength $M_{pl,N}$ and the (absolute value of) actual bending moment.

It seems interesting to plot (figure 11) the elastic contribution to the deflection: the effect of the constraints imposed in the three phases of the load process is evident. During analysis #1 the rotation at point A (abscissa $s = 0$) is free, while it is prevented in analysis #2: in the latter, the slope of the deflection curve at point A is constant and equal to 1^{deg}. The deflection at the end of analysis #2 is about 30% of the ultimate deflection. As expected therefore, most of the deflection takes place in analysis #3.

Table 2 allows to compare the performances of the props with and without the enlargement at the base. It shows that an enlargement of the bases of length $300mm$ allows to save about 4 kg, the 7.56% of the prop weight.

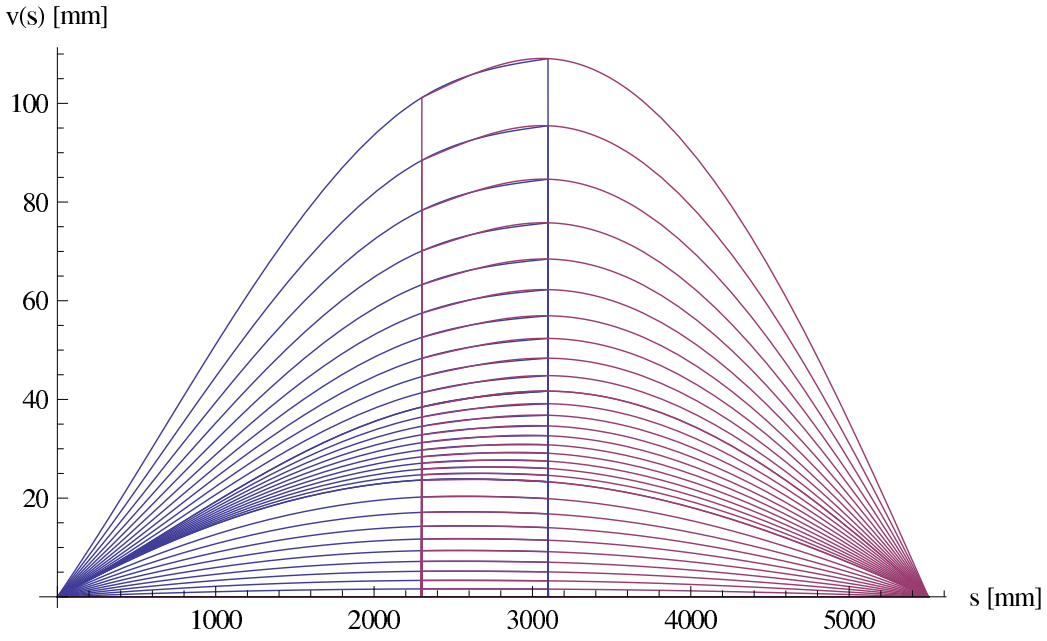

a)

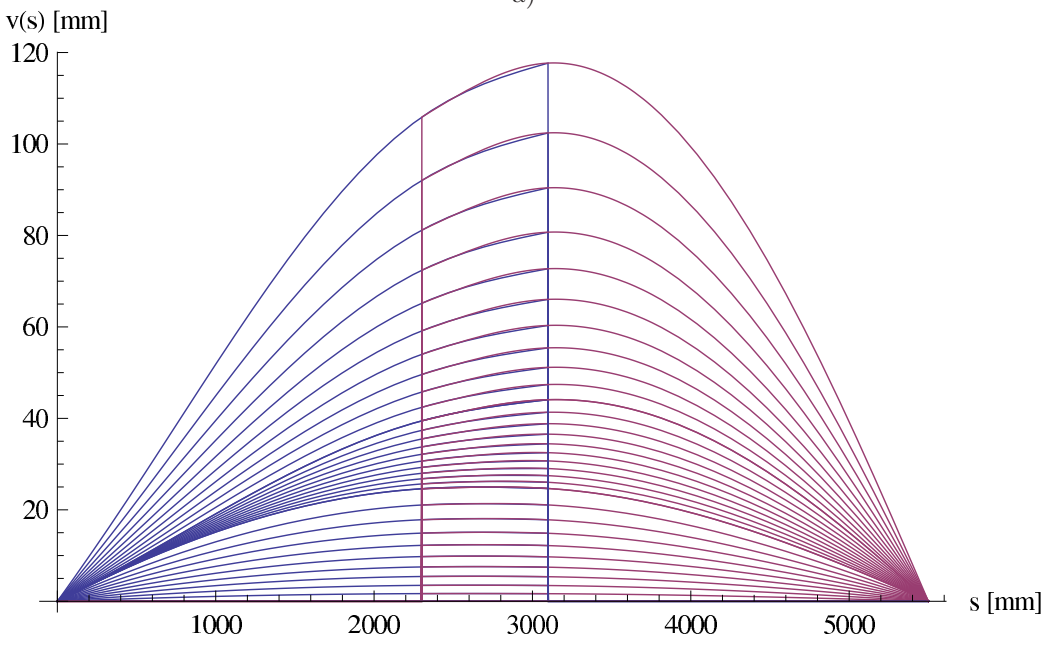

b)

Figure 11: Elastic deflection $v^{el}(s)\,[mm]$ as a function of the external load up to the carrying capacity P_{fail} for a standard prop (plot a)) and for an enlarged prop (plot b)). The latter is more compliant since the tubes are smaller.

5 Conclusions

The idea of lighter props of innovative shape arose from the evidence that the main failure mechanism for certain class of props is the failure of the base. In order to comply with the safety requirements against this collapse mechanism, it is usual in standard design to increment tube thicknesses. This methodology is only indirectly related to the failure mechanisms and causes a large increase of the prop weight. In the approach here pursued, the increment of thicknesses of the tubes is coupled with an enlargement of tube diameters near the prop base - see figure 4. Enlargement can be obtained by welding or by alternative technologies.

Prop type	Standard prop	Enlarged prop
$P_{1^{\deg}}$	11.78 kN	10.68 kN
P_{lim}	27.27 kN	27.24 kN
P_{fail}	34.43 kN	34.10 kN
$P_{cr,1}$	32.52 kN	31.06 kN
$P_{cr,2}$	61.73 kN	61.10 kN
$P_{cr,3}$	40.48 kN	39.15 kN
weight	49.47 kg	45.73 kg

Table 2: Comparison between a "standard" prop and an enlarged prop

The prop behavior can be modeled in either case as described in section 3.

The design of this new kind of prop required a deep revision of the strategy provided in [1], which is the main contribution of the present note. A new software has been developed to design props with enlarged bases, capable to optimize props in terms of weight.

Acknowledgments This work has been motivated and supported by the company Ferro-met S.r.l.: authors are grateful indebted with Dr. C. Boninsegna for his strong and warm cooperation.

References

[1] A. Salvadori. Ultimate strength of adjustable telescopic steel props according to standard EN 1065. *Journal of Constructional Steel Research*, 65:1964–1970, 2009.

A Evaluation of angle $\Delta\varphi_o$

The tolerances at the top and at the bottom between the two vertical tubes are defined as:

$$g_{bott} = d_o - d_p \; ; \qquad g_{top} = d_s - D_i$$

having set d_o the inner diameter of the outer tube and D_i the outer diameter of the inner tube. Moving from the vertical position, the tubes relatively rotate about the hinge in figure 6. Geometrical analysis lead to the following first order approximated (i.e. $\tan\varphi = \varphi$) equations:

$$\begin{cases} (l_o + l_m)\cdot\varphi_A - \frac{g_{top}}{2} = l_i \cdot \varphi_F \\ l_o \cdot \varphi_A = (l_i + l_m)\cdot\varphi_F - \frac{g_{bott}}{2} \end{cases} \tag{9}$$

whose solution yields φ_A and φ_F, whence $\Delta\varphi_o = \varphi_A + \varphi_F$.